Rat Adjuvant Arthritis: Imaging with Technetium-99m-Anti-CD4 Fab' Fragments

Raimund W. Kinne, Wolfgang Becker, Thomas Koscheck, Jürgen Kuhlmann, Robert M. Sharkey, Thomas Behr, Ernesta Palombo-Kinne, David M. Goldenberg, Friedrich Wolf and Frank Emmrich

Max-Planck-Society, Clinical Research Unit for Rheumatology/Immunology, Institute of Clinical Immunology and Rheumatology, Departments of Medicine III and Nuclear Medicine, University of Erlangen-Nuremberg, Erlangen, Germany; Max-Planck-Institute for Molecular Physiology, Department of Structural Biology, Dortmund, Germany; and Center of Molecular Medicine and Immunology, Newark, New Jersey

The abundance of CD4 molecules on inflammatory cells in the synovial membrane renders anti-CD4 monoclonal antibodies (MAbs) or their fragments very promising for specific imaging of arthritic joints. **Methods:** Joint uptake and body distribution of a ^{99m}Tc-labeled Fab', derived from the anti-rat CD4 MAb W3/25 (IgG_1), were investigated following intravenous injection in normal and adjuvant arthritic rats. An isotype-matched Fab' (anti-human nonspecific crossreacting antigen-90) was used as control. **Results:** A 14-hr sequential pinhole scan of the ankle joints revealed that both the anti-CD4 and the control Fab' accumulated to a higher degree in arthritic than in normal ankle joints; however, accumulation of the anti-CD4 Fab' in arthritic joints exceeded that of the control Fab' (~ 1.6 fold). Preferential joint accumulation of anti-CD4 Fab' was confirmed by whole-body scans at 14 hr and by direct well counter measurements of tissue samples at 16 hr following injection. Unlike the control Fab', the anti-CD4 Fab' preferentially accumulated in the liver and lymph nodes, organs rich in CD4-positive cells, as observed by direct tissue measurements. **Conclusion:** Despite its monovalency, the anti-CD4 Fab' retains the in vivo selectivity for CD4-positive cell-rich tissues, previously reported for the complete anti-CD4 MAb, and improves imaging of inflamed joints in experimental adjuvant arthritis.

Key Words: rat adjuvant arthritis; technetium-99m-anti-CD4 Fab' fragment; T-helper/inducer cells; macrophages

J Nucl Med 1995; 36:2268–2275

CD4-positive cells (i.e., the helper/inducer subset of T lymphocytes as well as macrophages) are abundant in the inflamed synovial membrane of human rheumatoid arthritis patients (*1–3*). A complete anti-CD4 monoclonal antibody (MAb) has recently proven effective in imaging inflamed rheumatoid arthritis joints (*4*). Although the target-to-background ratio with the complete anti-CD4 MAb was superior to that obtained with conventionally used polyclonal human immunoglobulin (HIG), the percentage of total-body counts accumulated in the inflamed joint was similar for the two tracers (*5,6*). Moreover, in rat adjuvant arthritis, an experimental arthritis model with histological similarities to human rheumatoid arthritis (*7–9*), both joint uptake and target-to-background ratio of a complete anti-rat CD4 MAb did not differ from those of an isotype-matched control (*10*). In this model, the target-bound fraction may have been obscured by nonspecific trapping of the complete anti-CD4 MAb due to its large size or by its binding to Fc-receptors in the inflamed synovial membrane. To verify this hypothesis, Fab' fragments of the above anti-rat CD4 MAb (W3/25; IgG_1)(*10*), smaller in size and lacking Fc parts, were produced and labeled with ^{99m}Tc and their joint uptake and body distribution in adjuvant arthritis rats were compared to those of Fab' fragments with irrelevant specificity (anti-human nonspecific crossreacting antigen-90; NCA-90).

MATERIALS AND METHODS

Animals

Induction of Adjuvant Arthritis. Female Lewis rats (body weight 133–218 g; age 7–10 wk) were injected intradermally into the tail base with 0.25 mg of heat-killed Mycobacterium tuberculosis (MT) in 0.1 ml paraffin oil. The degree of arthritis in each paw was graded from 0 to 4 according to the extent of erythema and edema (*11*). Arthritic rats were imaged on Day 19 of the disease (i.e., shortly before the clinical peak) (*12,13*). Only ankle joints with a minimum score of 2.5 were subjected to pinhole scans. The study was performed on 4 different groups of animals (n = 5 for each group): control rats received anti-NCA-90 Fab' or anti-CD4 Fab' and arthritic rats received anti-NCA-90 Fab' or anti-CD4 Fab'. The investigations were not performed on all animals in each group for reasons unrelated to the severity of arthritis.

To allow central venous application of the Fab' fragments, the external jugular vein was catheterized on the day of the experiment as previously described (*10,14*).

Received Oct. 5, 1994; revision accepted Apr. 12, 1995.

For correspondence or reprints contact: Raimund W. Kinne, MD, Institute of Clinical Immunology and Infusion Medicine, Delitzscher Strasse 141, D-04129 Leipzig, Germany.

Antibodies

The anti-rat-CD4 MAb (W3/25, IgG_1) is directed against the rat equivalent of the human CD4 molecule on both T-helper/inducer lymphocytes and macrophages (*15–17*). After purification of complete W3/25 MAbs from ascites as previously described (*18*), $F(ab')_2$ fragments were produced by pepsin digestion (2 hr at 37°C with 2.5 μg/ml pepsin in 0.035 *M* citrate buffer, pH 3.7). Size-exclusion HPLC (GF-250) was performed to monitor the progress of digestion. $F(ab')_2$ fragments were then purified by passage over a protein A column, ultrafiltrated and dialyzed against PBS.

$F(ab')_2$ fragments were then reduced (30 min at 37°C with 0.02 *M* cysteine in 0.002 *M* EDTA in 0.04 *M* PBS, pH 7.4) and changed into a 0.05 *M* sodium acetate buffer, pH 4.5, containing 0.15 *M* NaCl by using a PD-10 column (Pharmacia, Piscatway, NJ). The resulting Fab′ fragments were then formulated for direct labeling with ^{99m}Tc according to previously published methods (*19*), placed as a liquid into vials flushed with argon and stored frozen as a ready-to-label kit.

The affinity constants (K_A) of both the anti-CD4 Fab′ fragment and the complete anti-CD4 MAb were determined using soluble rat CD4 (*20*) and a BIAcore (Pharmacia Biosensor, AB, Uppsala, Sweden) surface plasmon resonance system (*21*).

The anti-human-NCA-90 MAb IMMU-MN3 (IgG_1; Immunomedics Inc., Morris Plains, NJ) (*22*) reacts with the nonspecific crossreacting-antigen-90 on the surface of human polymorphonuclear neutrophilic leukocytes (*22,23*). This control MAb did not show a positive immunohistochemical reaction on either cryostat sections of normal or inflamed rat synovial membrane or on rat blood smears (Kinne RW, *unpublished results*, 1994). Fab′ fragments of this MAb [affinity constant (K_A) $0.5 \pm 0.2 \times 10^8\ M^{-1}$ (*24*)] were produced, purified, prepared for radiolabeling as described above for the anti-rat CD4 Fab′ and provided as kits in lyophilized form.

Radiolabeling of Fab′ Fragments

Fab′ fragments (1.5 mg/ml) were incubated with 148 MBq ^{99m}Tc per mg Fab′. The percentages of protein-bound and free radioactivity were determined by gel chromatography over PD-10 columns (Pharmacia, Piscatway, NJ). The molecular weight of the radiolabeled proteins was analyzed by gel-filtration chromatography on Sephadex G-100 Superfine (Pharmacia) using purified Fab′ preparations as standards. Before injection, the total radioactivity of the injectant was determined.

Intravenous Injection and Imaging

After complete recovery from catheterization, rats were anesthetized with urethane (0.75 g/kg i.m.) and immobilized on a stretcher under a gamma camera. Two hundred and fifty micrograms (37 MBq) ^{99m}Tc-labeled anti-CD4 or control Fab′ were slowly injected intravenously. The accumulation of radiolabeled Fab′ fragments in the ankle joint was then followed in 15-min frames for 14 hr using a gamma camera equipped with a pinhole collimator and interfaced to a Micro-Delta computer system (Siemens, Erlangen, Germany). Integrated radioactivity distribution was measured using either 64×64 or 128×128 matrices.

Fourteen hours postinjection of the Fab′ fragments, whole-body scans were acquired using 10-min frames and matrices as above. For these scans, the gamma camera was fitted with a high-resolution, low-energy collimator.

Biodistribution of Fab′ Fragments

Sixteen hours after injection, organs, tissues and joints listed in Table 2 were excised after withdrawal of approximately 7–8 ml of blood. The tissue radioactivity was then counted in a well-type gamma scintillation counter. Values were expressed as the percent injected activity and per gram of wet weight of the samples (*10*).

Image Evaluation

Pinhole images of normal and arthritic ankle joints were evaluated by placing a region of interest (ROI) over the ankle joint and a reference region of equal size over the immediately adjacent lower leg. Data were expressed as counts accumulated in the two regions during time frames of 15 min, corrected for ^{99m}Tc decay, or as the ratio between radioactivity levels in the ROI and those in the reference region. In addition, the radioactivity accumulated in the ankle and wrist joints 14 hr after injection of the Fab′ fragments was determined by placing ROIs over the joints on the whole-body scans. Values were expressed as the percentage of injected radioactivity.

Plasma Clearance of Technetium-99m-Labeled Fab′ Fragments

Timed arterial blood samples (approximately 50 μl; every 10 sec during the first minute, then at 1, 1.5, 2, 3, 5, 15, 25, 45, 60, 90, 120 min and every 60 min from 3–14 hr) were drawn from catheterized carotid arteries in separate groups of rats ($n = 3$ for the anti-NCA-90 Fab′; $n = 4$ for the anti-CD4 Fab′) and centrifuged. The radioactivity contained in the plasma (20 μl) and blood cells was measured separately in a well counter.

Statistical Analysis

A nonparametric test (Kruskall-Wallis test) was used to compare the radioactivity values of the two different Fab′ fragments in tissue preparations. Due to the high number of comparisons, $p \leq 0.01$ was considered significant. Organs and tissues showing significant differences in this test were then analyzed for differences among groups by the Mann-Whitney (U) test, with $p \leq 0.05$ indicating significant differences. The latter test and significance level were also applied for the results of pinhole and whole-body imaging, as well as for the analysis of plasma levels of Fab′ fragments. Correlations between clinical scores and the accumulation of radioactivity in individual arthritic joints in whole-body scans were analyzed using the Spearman-Rank correlation. Statistical significance was $p \leq 0.05$.

RESULTS

Radiopharmaceuticals Quality Control

Both Fab′ preparations contained less than 4% free pertechnetate 15 min after radiolabeling (Fig. 1). In addition, more than 91% of the radiolabel was attached to protein with an apparent molecular weight of 55 kD, which presumably represented Fab′ fragments (Fig. 2). The remaining radioactivity was attached to molecules with a larger molecular weight, presumably $F(ab')_2$ fragments (Fig. 2).

Clinical Scores of Rats with Adjuvant Arthritis

There were no significant differences between the clinical scores of animals receiving the anti-CD4 [1.75 ± 0.33 fore paws; 3.46 ± 0.23 hind paws (mean ± s.e.m.)] or the anti-NCA-90 Fab′ (2.29 ± 0.33 fore paws; 3.33 ± 0.19 hind paws). Control animals showed no signs of joint inflammation.

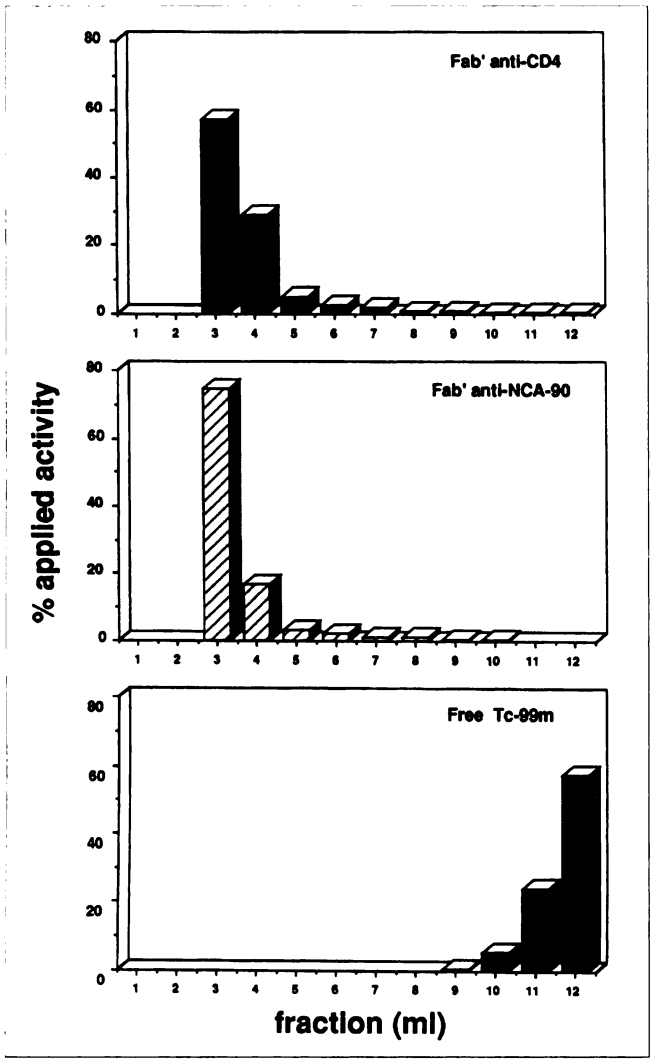

FIGURE 1. Gel chromatography of Fab' fragments on a PD-10 column 15 min following radiolabeling with ^{99m}Tc. Radiopharmaceuticals were eluted with 0.9% NaCl in 1-ml fractions. Both Fab' fragment preparations contain less than 4% free ^{99m}Tc.

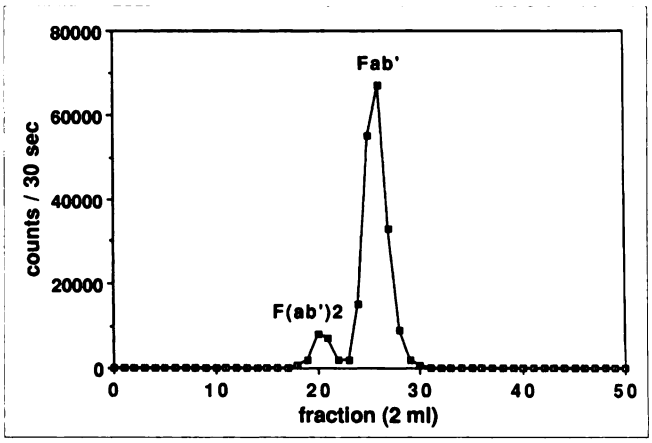

FIGURE 2. Gel chromatography of anti-CD4 Fab' fragments on a Sephadex G-100 Superfine column 15 min after radiolabeling with ^{99m}Tc. Radiopharmaceuticals were eluted with 0.9% NaCl in fractions of 2 ml/15 min. More than 91% of the radiolabel is attached to Fab' fragments and the remaining activity to $F(ab')_2$ fragments.

Plasma Clearance

Maximal arterial plasma concentration of both anti-CD4 and control Fab' fragments was reached within 10 sec following bolus injection into the central venous catheter (Fig. 3). Plasma levels of the anti-NCA-90 Fab' remained higher compared to those of the anti-CD4 Fab', with significant differences at 1, 2, 45, 60 and 90 min, and 2, 3, 4 and 7 hr following intravenous injection.

Pinhole Gamma Camera Scanning of Ankle Joints

Anti-CD4 Fab'. The levels of radioactivity in the arthritic ankle joint showed a maximum at 45 min, while those in the reference region peaked 15 min after i.v. injection of the labeled anti-CD4 Fab' (Fig. 4B). The anti-CD4 Fab' accumulated to a greater extent in arthritic ankle joints (Fig. 4B) than in noninflamed ankle joints (Fig. 4D). More importantly, the accumulation of the anti-CD4 Fab' in the arthritic ankle joint was higher than that of the control Fab' throughout the 14-hr experimental period (Fig. 4A, B). The differences between the two tracers were confirmed when the data were expressed as ratios between the ROI (arthritic ankle joint) and the reference region (lower leg; Fig. 5). The ratios for the anti-CD4 Fab' were significantly higher than those for the control Fab' from 15 min until 12.5 hr postinjection (Fig. 5). Representative gamma camera images, obtained 5 hr postinjection, of normal and arthritic ankle joints, are shown in Figure 6.

A limited accumulation was observed in the distal lower leg adjacent to inflamed joints for both the anti-CD4 and the control Fab' (Fig. 4).

In the control rats, the accumulation of anti-CD4 Fab' in both the ankle joint and lower leg (Figs. 4D, 5) was similar to that of anti-NCA-90 Fab' (Figs. 4C, 5).

Anti-human NCA-90 Fab'. The levels of control Fab' in the arthritic ankle joint increased until 1 hr after injection and decreased thereafter (Fig. 4A). The levels were higher in arthritic than in normal ankle joints (Fig. 4A, C) but lower in arthritic joints than in the case of the anti-CD4 Fab' throughout the experiment (Figs. 4A, B, 5). Representative gamma camera images obtained 5 hr after tracer injection are shown in Figure 6.

Whole-body Gamma Camera Scanning

The results of whole-body scanning in the control and arthritic rats are shown in Table 1.

Anti-CD4 Fab'. In the wrist joints, there were no significant differences between arthritic and control rats or between anti-CD4 and control Fab' fragments. In contrast, the accumulation of anti-CD4 Fab' in arthritic ankle joints was significantly higher than that in normal ankle joints ($p < 0.05$). More importantly, the accumulation of anti-CD4 Fab' in arthritic ankle joints was higher than that of control Fab' ($p < 0.05$; Table 1).

Anti-human NCA-90 Fab'. No significant differences were present in the wrist joints. The accumulation of anti-NCA-90 Fab' in arthritic ankle joints was significantly higher than that in normal ankle joints ($p < 0.05$; Table 1)

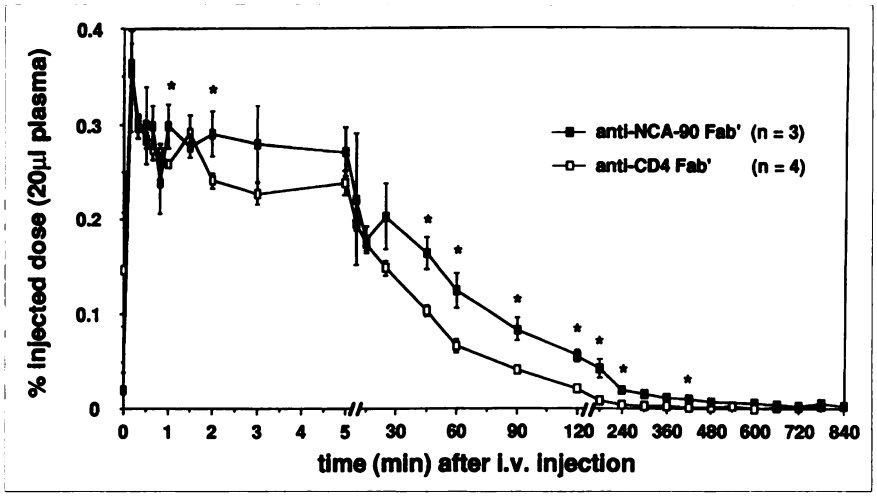

FIGURE 3. Arterial plasma clearance of anti-NCA-90 and anti-CD4 Fab' fragments in arthritic animals (means ± s.e.m.; *p ≤ 0.05). Plasma levels of the anti-CD4-Fab' are significantly lower than those of the control Fab' at most time points within 7 hr following injection.

but significantly lower than that of the anti-CD4 Fab' (Table 1).

The accumulation of radioactivity in arthritic joints after injection of either anti-CD4 or control Fab', as determined in whole-body scans, showed a highly significant correlation with the clinical scores of individual joints [$p < 0.0001$ for all animals ($n = 10$); $p = 0.003$ for animals injected with anti-CD4 Fab' ($n = 5$); $p = 0.03$ for animals injected with the control Fab' ($n = 5$)].

Body Distribution

The results are summarized in Table 2.

Anti-CD4 Fab'. Sixteen hours following intravenous injection, the highest activity was observed in the kidneys,

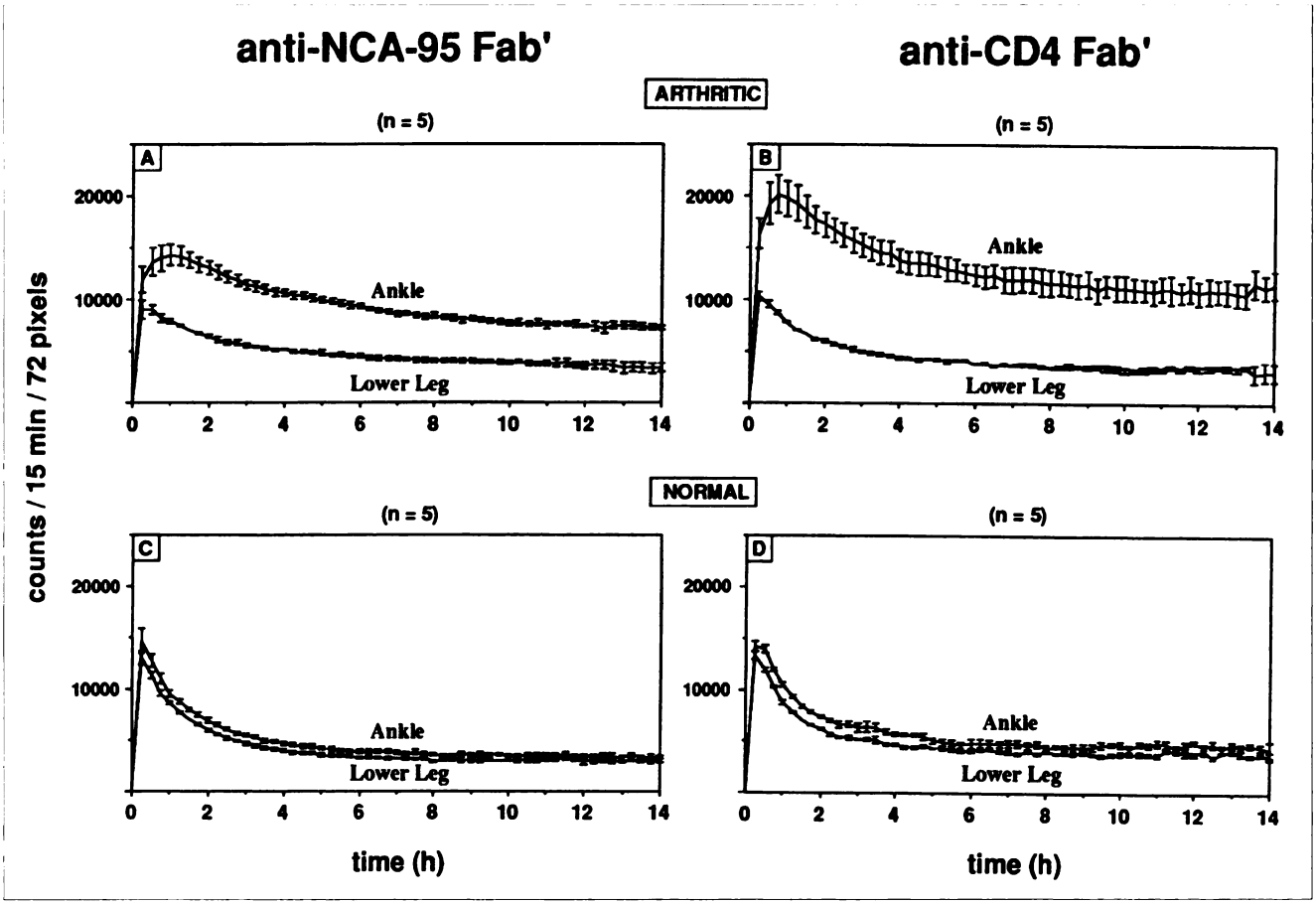

FIGURE 4. Joint uptake of anti-NCA-90 (A,C) and anti-CD4 Fab' (B,D) in the ankle joints (ROI) and lower legs (reference region) of arthritic (A,B) or control (C,D) rats after intravenous injection (means ± s.e.m.). Accumulation of anti-CD4 Fab' in arthritic ankle joints is consistently higher than that of control Fab'.

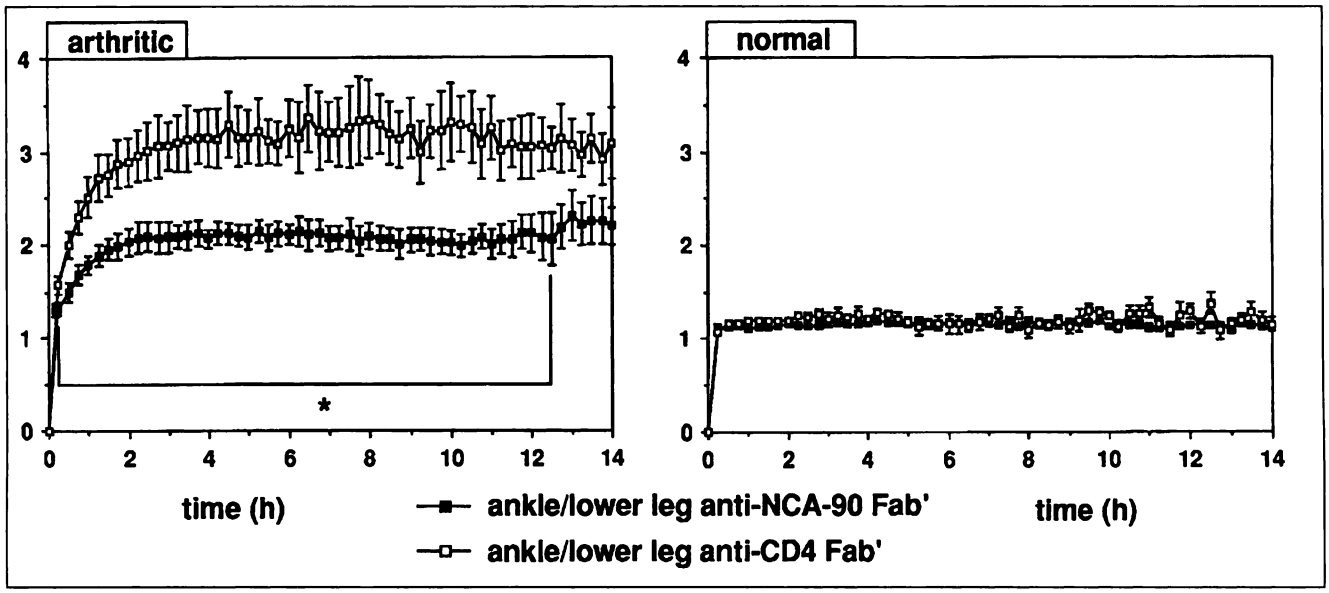

FIGURE 5. Ratio between ankle joints and lower legs following intravenous injection of anti-NCA-90 and anti-CD4 Fab' fragments in arthritic (left panel) and control rats (right panel; means ± s.e.m.; *$p \leq 0.05$). Ratios obtained in arthritic joints for anti-CD4 Fab' are consistently higher than those for the control Fab'.

with no significant differences between arthritic and control rats or between anti-CD4 and control Fab'.

Arthritic rats showed significantly higher levels of the anti-CD4 Fab' in the liver and ankle joints than the controls ($p \leq 0.05$; Table 2).

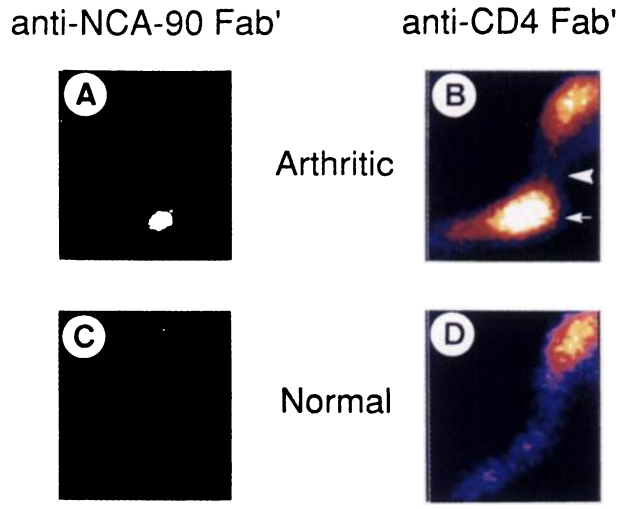

FIGURE 6. Gamma camera images of the ankle joint (arrow) and lower leg (arrowhead) of arthritic (A,B) and control (C,D) rats 5 hr after intravenous injection of anti-NCA-90 Fab' (A,C) or anti-CD4 Fab' (B,D). Colors represent levels of radioactivity ranging from low (blue) to high (white). The accumulation of both Fab' fragments is higher in arthritic (A,B) than in the normal ankle joints (C,D), but anti-CD4 Fab' (B) shows higher levels in arthritic ankle joints than anti-NCA-90 control Fab' (A). This is also true for the knee joint (B upper right corner), which is frequently involved in the arthritic process. In normal knee joints (C,D), target-to-background ratios between the knee joint and adjacent reference region (lower leg) were not significantly different for the two Fab' fragments (data not shown).

Anti-CD4 Fab' demonstrated highly selective accumulation (i.e., significantly higher than that of the control Fab') in lymphoid organs rich in CD4-positive cells such as mesenteric, submandibular and inguinal lymph nodes, but not in the spleen ($p = 0.047$; Kruskall-Wallis test) in both the control and arthritic animals (Table 2). Preferential accumulation of anti-CD4 Fab' also occurred in the liver and, most notably, in the inflamed ankle joints (Table 2).

In both normal and arthritic animals, anti-CD4 Fab' displayed significantly lower whole blood and plasma radioactivity levels than the control Fab' (Table 2).

Anti-NCA-90 Fab'. For this Fab', the ankle joint and the mesenteric lymph nodes of arthritic rats were the only sites in which differences of accumulated radioactivity attained statistical significance in comparison to controls (Table 2).

TABLE 1
Accumulation of Anti-Human-NCA-90 or Anti-Rat-CD4 Fab' Fragments in Normal and Arthritic Ankle Joints (Whole-body Scans)

	Control rats		Arthritic rats	
Joints*	Anti-NCA-90 (n = 4)	Anti-CD4 (n = 4)	Anti-NCA-90 (n = 4)	Anti-CD4 (n = 4)
Wrists	0.04 ± 0.01	0.05 ± 0.00	0.06 ± 0.01	0.07 ± 0.01
Ankles	0.06 ± 0.01	0.08 ± 0.01	0.30 ± 0.04†	0.55 ± 0.06†‡

*Values of left and right joints were added. Data are expressed as the percent of injected activity 14 hr following intravenous injection (means ± s.e.m.) for the number of animals indicated in parentheses.

†$p < 0.05$ Mann-Whitney U-test for comparison between control and arthritic rats for the same Fab' fragment.

‡$p < 0.05$ Mann-Whitney U-test for comparison between anti-NCA-90 and anti-CD4 Fab' fragments in arthritic and normal animals.

TABLE 2
Whole-Body Distribution of Anti-Human NCA-90 Fab' and Anti-CD4 Fab' in Control and Arthritic Rats

Tissue	Control rats		Arthritic rats	
	Anti-NCA-90 (n = 4)	Anti-CD4 (n = 4)	Anti-NCA-90 (n = 4)	Anti-CD4 (n = 4)
Thymus	0.13 ± 0.01	0.12 ± 0.01	0.19 ± 0.02	0.12 ± 0.01
Lungs	0.31 ± 0.04	0.44 ± 0.10	0.17 ± 0.01	0.34 ± 0.03
Liver	0.50 ± 0.06	1.06 ± 0.03†	0.54 ± 0.06	1.28 ± 0.07*†
Spleen	2.06 ± 0.35	2.63 ± 0.25	1.58 ± 0.25	2.96 ± 0.26
Intestine (small)	0.37 ± 0.04	0.78 ± 0.17	0.33 ± 0.06	0.52 ± 0.09
Intestine (large)	0.07 ± 0.03	0.53 ± 0.29	0.03 ± 0.00	0.04 ± 0.00
Feces	0.44 ± 0.40	0.30 ± 0.14	0.12 ± 0.07	0.03 ± 0.01
Kidneys	27.71 ± 1.17	27.44 ± 1.47	15.19 ± 5.46	28.18 ± 1.88
Blood (whole)	0.13 ± 0.02	0.05 ± 0.01†	0.13 ± 0.02	0.05 ± 0.01†
Blood cells	0.05 ± 0.02	0.04 ± 0.01	0.05 ± 0.01	0.04 ± 0.01
Plasma	0.20 ± 0.03	0.05 ± 0.02†	0.16 ± 0.02	0.09 ± 0.01†
Bone marrow	0.12 ± 0.03	0.12 ± 0.02	0.09 ± 0.03	0.14 ± 0.03
Peyer's plaques	0.29 ± 0.04	0.61 ± 0.05	0.29 ± 0.08	0.47 ± 0.05
Mesenteric ln.	0.15 ± 0.01	0.68 ± 0.08†	0.21 ± 0.02*	0.62 ± 0.03†
Submandibular ln.	0.28 ± 0.05	0.58 ± 0.03†	0.26 ± 0.04	0.41 ± 0.02*†
Axillar ln.	0.19 ± 0.05	0.48 ± 0.06	0.24 ± 0.06	0.31 ± 0.05
Subscapular ln.	0.19 ± 0.02	0.41 ± 0.04	0.19 ± 0.02	0.25 ± 0.06
Inguinal ln.	0.12 ± 0.03	0.36 ± 0.04†	0.18 ± 0.03	0.28 ± 0.01†
Popliteal ln.	0.16 ± 0.05	0.50 ± 0.20	0.25 ± 0.03	0.26 ± 0.02
Retroperitoneal ln.	0.29 ± 0.11	0.71 ± 0.09	0.31 ± 0.02	0.34 ± 0.04
Toes	0.08 ± 0.01	0.08 ± 0.00	0.07 ± 0.01	0.10 ± 0.01
Ankles	0.06 ± 0.01	0.06 ± 0.00	0.13 ± 0.02*	0.20 ± 0.02*†
Knees	0.12 ± 0.01	0.15 ± 0.01	0.11 ± 0.02	0.22 ± 0.03
Fingers	0.06 ± 0.01	0.09 ± 0.01	0.08 ± 0.01	0.11 ± 0.02
Wrists	0.07 ± 0.01	0.07 ± 0.01	0.10 ± 0.02	0.11 ± 0.03
Elbows	0.06 ± 0.01	0.06 ± 0.00	0.05 ± 0.01	0.08 ± 0.01
Skin	0.05 ± 0.01	0.06 ± 0.00	0.04 ± 0.00	0.05 ± 0.01
Muscle	0.02 ± 0.01	0.01 ± 0.00	0.04 ± 0.01	0.03 ± 0.01
Synovia	n.d.	n.d.	0.21 ± 0.03	0.29 ± 0.04

*$p \leq 0.05$ Mann-Whitney U-test for comparison between controls and arthritic rats for the same Fab' fragment.
†$p \leq 0.05$ Mann-Whitney U-test for comparison between anti-NCA-90 and anti-CD4 Fab' fragments in arthritic and control rats.
Values of the left and right sides of bilateral tissues or organs were added. ln. = lymph nodes; n.d. = not determined. Data are expressed as the percent injected activity per gram of sample wet weight (means ± s.e.m.) 16 hr after intravenous injection for the number of animals indicated in parentheses.

Affinity Constants (K_A) of Anti-CD4 Fab' and Complete Anti-CD4 MAb.

The K_A values of anti-CD4 Fab' and the complete anti-CD4 MAb were 1.15×10^9 M^{-1} and 0.42×10^9 M^{-1}, respectively.

DISCUSSION

The present study shows that anti-CD4 Fab' accumulates in arthritic joints to a significantly higher degree than the control Fab' (Figs. 4, 5, 6; Tables 1 and 2). This represents a clear improvement over the performance of a complete anti-CD4 MAb, which showed no preferential accumulation in arthritic joints in comparison to an isotype-matched MAb (*10*). The binding of the anti-CD4 Fab' to target CD4-molecules present on joint inflammatory cells, although monovalent in comparison to the complete anti-CD4 MAb, may therefore be sufficient to attain specific imaging. Indeed, the affinity constants (K_A) of the complete anti-CD4 MAb and its Fab' counterpart are of the same order of magnitude. Therefore, comparison of the performance of the two molecules appears justified.

The improved performance of anti-CD4 Fab' may be explained by the fact that Fc parts, which could bind to Fc receptors abundant on inflammatory cells in arthritic joints (*25*), are lacking in this molecule. In addition, the small size of anti-CD4 Fab' may facilitate faster washout of the unbound fraction, which in turn may have obscured specific binding in the case of the large, complete anti-CD4 MAb (*10*).

The increased entry of both specific and control Fab' into arthritic joints is likely due to higher permeability of the inflamed endothelium for large proteins (*26*), as reflected in the ratio between the inflamed ankle joint and the reference region for the control Fab' (~2; Fig. 5). On the other hand, the favorable accumulation of the specific anti-CD4 in comparison to the nonspecific control Fab' indicates that the immunological specificity of the anti-CD4

Fab′ may significantly contribute to its retention in the inflamed joint.

A time point as early as 4 hr postinjection of anti-CD4 Fab′ seems to already provide an optimal target-to-background ratio for the arthritic joint. This ratio, in fact, remained essentially constant after reaching a plateau 4 hr following injection (Fig. 5).

For anti-CD4 Fab′, there was excellent correlation ($p = 0.003$) between levels of joint radioactivity in the whole-body scans and clinical scores in individual inflamed joints. This correlation was significant at a lower level ($p = 0.03$) for the control Fab′ but was completely absent in the case of complete anti-CD4 MAb (*10*). In experimental adjuvant arthritis, imaging with Fab′ fragments appears to be a reliable measure of the actual inflammatory activity in arthritic joints.

For anti-CD4 Fab′, the plasma radioactivity levels were significantly lower than those of the control Fab′ for 7 hr after injection of the agents (Fig. 3; Table 2). This finding may be due to extraction of the anti-CD4 Fab′ from the circulation by tissues rich in CD4-positive-cells, a phenomenon that does not occur with the control Fab′ (Table 2) but has already been observed with the complete anti-CD4 MAb (*10*). Lower plasma levels of the anti-CD4 Fab′ may also thus contribute to the improved target-to-background ratio in the inflamed joint.

The accumulation of anti-CD4 Fab′ in lymph nodes and liver, even in the control animals, appears to reflect its selectivity for organs and tissues rich in CD4-positive cells. This property may be suitable for identifying lesions such as extramedullary infiltrations of lymphocytic or myelogenous leukemias (*27*).

In liver and mesenteric lymph nodes of arthritic animals, the accumulation of either specific or control Fab′ was higher than that in normal rats (Table 2). This may reflect augmented nonspecific permeability in these structures, conceivably related to the systemic inflammatory character of the adjuvant arthritis model (*28*).

Both anti-CD4 and control Fab′ fragments showed higher radioactivity levels in the kidneys and shorter plasma half-lives than the respective complete MAbs (*10*) (Table 2). This appears to be caused by higher excretion through the kidneys (Kinne RW, *unpublished observations*, 1995), as expected on the basis of the smaller size of the Fab′ fragments.

CONCLUSION

These findings suggest that anti-CD4 Fab′ fragments are valuable tools for imaging arthritic joints. Their properties—selective imaging of inflammatory infiltrates, correlation of joint accumulation with clinical activity and achievement of optimal imaging conditions at 4 hr postinjection—render anti-CD4 Fab′ fragments very promising for determining actual inflammatory activity in experimental as well human arthritis.

ACKNOWLEDGMENTS

The authors thank J. Harzendorf and F. Kübel for expert technical assistance and Dr. M. Meyer, Institute for Medical Statistics and Documentation, University of Erlangen-Nuremberg for advice on statistical analysis. The Max-Planck-Society, Clinical Research Unit for Rheumatology/Immunology, is funded by the German Ministry for Research and Technology (BMFT grant FKZ 01 VM 8702).

REFERENCES

1. Burmester GR, Yu DTY, Irani AM, Kunkel HG, Winchester RJ. Ia+ T cells in synovial fluid and tissue of patients with rheumatoid arthritis. *Arth Rheum* 1981;24:1370–1376.
2. Janossy G, Duke O, Poulter LW, Panayi G, Bofill M, Goldstein G. Rheumatoid arthritis: A disease of T-lymphocyte/macrophage immunoregulation. *Lancet* 1981;839–842.
3. Kinne RW, Becker W, Schwab J, et al. Imaging of arthritic joints with technetium-99m-labeled immunoglobulins—comparison of specific anti-CD4 monoclonal antibodies with nonspecific immunoglobulins. In: Fritsch J, Mueller-Peddinghaus R, eds. *Advances in rheumatology and inflammation*, Vol. 2. Basel: Euler Publishing; 1992:161–174.
4. Becker W, Emmrich F, Horneff G, et al. Imaging rheumatoid arthritis specifically with technetium-99m-CD4-specific (T-helper lymphocytes) antibodies. *Eur J Nucl Med* 1990;17:156–159.
5. Kinne RW, Becker W, Schwab J, et al. Comparison of ^{99m}Tc-labeled specific murine anti-CD4 monoclonal antibodies and nonspecific human immunoglobulin for imaging inflamed joints in rheumatoid arthritis. *Nucl Med Commun* 1993;14:667–675.
6. Kinne RW, Becker W, Schwab J, et al. Comparison of ^{99m}Tc-labeled specific murine anti-CD4 monoclonal antibodies and nonspecific human immunoglobulin for imaging inflamed joints in rheumatoid arthritis. *Orth Rheumatol Dig* 1994;8:7–8.
7. Pearson CM, Wood FD. Studies of arthritis and other lesions induced in rats by the injection of mycobacterial adjuvant. VII. Pathologic details of the arthritis and spondylitis. *Am J Pathol* 1963;42:73–95.
8. Taurog JD, Argentieri DC, Reynolds RA. Adjuvant arthritis. *Meth Enzymol* 1988;162:339–355.
9. Billingham MEJ, Hicks C, Carney S. Monoclonal antibodies and arthritis. *Agents Actions* 1990;29:77–87.
10. Kinne RW, Becker W, Simon G, et al. Joint uptake and body distribution of a technetium-99m-labeled anti-rat CD4 monoclonal antibody in rat adjuvant arthritis. *J Nucl Med* 1993;34:92–98.
11. Wood FD, Pearson CM, Tanaka A. Capacity of mycobacterial wax D and its subfractions to induce adjuvant arthritis in rats. *Int Arch Allergy* 1969;35:456–467.
12. Pearson CM. Development of arthritis, periarthritis and periostitis in rats given adjuvants. *Exp Biol Med* 1956;91:95–101.
13. Pearson CM, Wood FD. Studies of arthritis and other lesions induced in rats by the injection of mycobacterial adjuvant. *Am J Pathol* 1963;42:73–95.
14. Bodziony J, Schwille PO. Subcutaneous cannula in the jugular and femoral vein—a tool for frequent blood sampling and infusions in the rat. *Z Versuchstierk* 1985;27:29–32.
15. Williams AF, Galfre G, Milstein C. Analysis of cell surfaces by xenogeneic myeloma-hybrid antibodies: differentiation antigens of rat lymphocytes. *Cell* 1977;12:663–668.
16. White RAH, Mason DW, Williams AF, Galfre C, Milstein C. T-lymphocyte heterogeneity in the rat: separation of functional subpopulations using a monoclonal antibody. *J Exp Med* 1978;148:664–669.
17. Jefferies WA, Green JR, Williams AF. Authentic T helper CD4 (W3/25) antigen on rat peritoneal macrophages. *J Exp Med* 1985;162:117–127.
18. Guse AH, Milton AD, Schulze-Koops H, et al. Purification and analytical characterization of an anti-CD4 monoclonal antibody for human therapy. *J Chromatog* 1994;661:13–23.
19. Hansen HJ, Jones AL, Sharkey RM, et al. Preclinical evaluation of an instant Tc-99m-labeling kit for antibody imaging. *Cancer Res* 1990;50:794–798.
20. Davis SJ, Ward HA, Puklavec MJ, Willis AC, Williams AF, Barclay AN. High level expression in chinese hamster ovary cells of soluble forms of CD4 T lymphocyte glycoprotein including glycosylation variants. *J Biol Chem* 1990;265:10410–10418.
21. Karlsson R, Michaelsson A, Mattson L. Kinetic analysis of monoclonal antibody-antigen interactions with a new biosensor based analytical system. *J Immunol Meth* 1991;145:229–240.

22. Hansen HJ, Goldenberg DM, Newman ES, Grebenau R, Sharkey RM. Characterization of second generation monoclonal antibodies against carcinoembryonic antigen. *Cancer* 1993;71:3478–3485.
23. Berling B, Kolbinger F, Grunert F et al. Cloning of carcinoembryonic antigen family member expressed in leukocytes of chronic myeloid leukemia patients and bone marrow. *Cancer Res* 1990;50:6534–6539.
24. Becker W, Bair J, Behr T, et al. Detection of soft-tissue infections and osteomyelitis using a technetium-99m-labeled anti-granulocyte monoclonal antibody fragment. *J Nucl Med* 1994;35:1436–1443.
25. Bröker BM, Edwards JCW, Fanger M, Lydyard PM. The prevalence and distribution of macrophages bearing FcγRI, FcγRII and FcγRIII in synovium. *Scand J Rheumatol* 1990;19:123–135.
26. Kushner I, Somerville JA. Permeability of human synovial membrane to plasma proteins. *Arth Rheum* 1971;14:560–570.
27. Carrasquillo JA, Bunn PA, Keenan AM, et al. Radioimmunodetection of cutaneous T-cell lymphoma with ^{111}In-labeled T101 monoclonal antibody. *N Engl J Med* 1986;315:673–680.
28. Billingham MEJ. Models of arthritis and the search for anti-arthritic drugs. In: Orme MCLE, ed. *Anti-rheumatic drugs*. New York: Pergamon Press; 1990:1–47.